Numerical Modelling of Wave and Tidal Current Interactions and Their Impact on Wave Parameters

Tian Tan, Vengatesan Venugopal

Abstract—**In regions where both waves and tidal currents coexist, tidal flow can significantly alter wave parameters and hence affects the estimation of wave energy resources. This study uses a coupled wave-current numerical model to evaluate the influence of wave-current interactions on wave parameters. To achieve this, the simulation was performed in 3 stages. At first, a large-scale North Atlantic wave model was constructed using the spectral wave model TOMAWAC to generate wave conditions and boundary inputs. This wave model was calibrated and validated at four sites around the UK using field measurements. Secondly, a tidal flow model for a small-scale region covering the Pentland Firth and Orkney Waters, Scotland, UK, was chosen, and tidal currents were simulated by the three-dimensional flow model TELEMAC 3D. As with the wave model, the flow model was also calibrated and validated with site measurements from an Acoustic Doppler Current Profiler (ADCP). In the third stage, a coupled TOMAWAC-TELEMAC 3D model was employed for the small-scale region, and the wave parameters generated by the large-scale model were input as boundary conditions. The TOMAWAC-TELEMAC 3D coupled model was validated with field measurements at two locations in Orkney Waters, where waves and currents coexist. Various wave and tidal currents parameters produced from the coupled model are presented in the paper. To evaluate the wave-current impact on wave parameters, a qualitative and quantitative analysis of these parameters is carried out, and the results are presented and discussed in the paper.**

Keywords—**spectra wave model, tidal flow model, TOMAWAC, TELEMAC 3D, wave-current interactions.**

The authors are grateful for financial support from the UK Engineering and Physical Sciences Research Council through CableDyn: Subsea Power Cable Dynamics Under Complex Ocean Environment (EP/W015102/1). The authors acknowledge support from the SIMEC Atlantis Energy (MyGen project) for providing ADCP data.

Tian Tan (e-mail: tian.tan@ed.ac.uk) and Vengatesan Venugopal (e-mail: V.Venugopal@ed.ac.uk) are with Institute for Energy Systems, School of Engineering, The University of Edinburgh at Sanderson Building, Robert Stevenson Road, The King's Buildings, Edinburgh, EH9 3FB, UK.

Digital Object Identifier: https://doi.org/10.36688/ewtec-2023-279

I. INTRODUCTION

Scotland is globally recognized as a prominent location for the development of marine energy technologies, specifically for wave and tidal current energies. This is due to the geographical advantage of the western coast of the Scotland, which faces the North Atlantic and experiences predominantly south-westerly winds, resulting in significant and consistent swell waves. Meanwhile, the numerous islands in northern Scotland have shaped a large number of waterways or channels, which are prone to high-speed tidal currents. Taken together, these environment conditions make Scotland, and especially the Pentland Firth and Orkney Waters (PFOW) in the north, a strong resource of wave and tidal energy.

The aforementioned geographical features of the PFOW region dictate a strong coexistence of waves and currents, making wave-current interactions inevitable and significant. It is widely acknowledged that the presence of fast tidal currents can alter surface waves, leading to a considerable increase or decrease in wave heights. Consequently, an inaccurate wave resource assessment of the PFOW areas can result from the failure to account for wave-current interaction effects. Moreover, wave-current interactions can increase the turbulence levels of tidal flow, resulting in unstable fluid environments that create operational challenges for tidal turbines. Therefore, comprehending the impact of wave-current interactions on wave and current parameters is critical for the successful development of marine energy in PFOW regions.

Numerical modelling is a commonly used method to study waves and tides. Since these phenomena are distinct from each other, they are typically simulated separately using different software. To simulate ocean waves in the PFOW region, the SWAN [1], [2] and MIKE 21 [3] spectral wave models have been utilized. Meanwhile, for tidal flow simulations, researchers have employed two-dimensional flow models, such as DG-ADCIRC [4] and TELEMAC 2D [5], and three-dimensional flow models, such as 3D SUNTANS [6], MIKE 3 [7], 3D ROMS [8], DELFT 3D [7], [9], TELEMAC

3D [9], and 3D FVCOM [10] to assess tidal energy resources and study impact of energy extraction on the environment. However, previous studies have not considered wave-current interactions as they only simulated waves or tidal currents alone. To address this limitation, Saruwatari et al. used SWAN and MOHID to model the wave-current coupling and studied the impact of wave-current interaction on wave power prediction [11]. However, the resolution of the model limited the accuracy of the model calibration and verification, indicating a need for further improvement. Additionally, Venugopal and Nemalidinne developed a high-resolution coupling model using MIKE 21 and MIKE 3 [12], [13], with wave boundary conditions extracted from the North Atlantic scale wave model [3]. This model demonstrated strong potential in accurately evaluating both wave and tidal energy resources. While the drawback is that MIKE is a commercial software, which requires users to purchase a license, thus restricting the use of cost-free software.

This study employs both the TOMAWAC wave spectra model [14] and the TELEMAC 3D three-dimensional flow [15] model to simulate wave and tidal flow parameters with wave-current interactions. These models are submodules of the open-source finite element computer program suite TELEMAC-MASCARET system [16], of which TELEMAC 3D has previously demonstrated success in the study of the PFOW region [9]. In contrast, TOMAWAC has not been used in PFOW to the best of the author's knowledge but has been proven effective in wave parameter predicting in many other cases [17].

The first step of this study involved using TOMAWAC to build a North Atlantic-scale wave model to generate accurate wave boundary conditions for subsequent smaller-scale models. Subsequently, a TELEMAC 3D flow model covering the whole PFOW area was constructed and coupled with TOMAWAC which utilize the same geometric mesh. The models were calibrated and validated using field measurements of wave buoys and Acoustic Wave and Current Profiler (AWAC)/ Acoustic Doppler Current Profiler (ADCP) data. By comparing the model simulations, the impact of wave-current interaction can be analysed qualitatively and quantitatively.

II. METHODOLOGY

A. Field Data Description

The calibration and validation of the wave model utilized four buoys from the Cefas WaveNet wave monitoring network [18], located in Scotland's waters, as reference points. Table I presents detailed information regarding these buoys, while Fig. 1 shows their locations. Notably, these buoys were chosen because wave-current interactions were negligible due to the low current speeds in the open sea. Therefore, the buoys serve as an optimal data source for validating the North Atlantic-scale TOMAWAC wave models in the absence of currents.

TABLE I
DETAILS OF CEFAS WAVENET BUOYS USED FOR NORTH-ATLANTIC SCALE TOMAWAC MODEL CALIBRATION AND VALIDATION

Site	Latitude	Longitude	Water depth
Hebrides	57°17'.53 N	7°54'.85 W	100 m
Blackstone	56°03'.73 N	7°03'.41 W	97 m
Moray Firth	57°57'.99 N	3°19'.99 W	54 m
Firth of Forth	56°11'.27 N	2°30'.24 W	65 m

The flow model and wave-current coupled model are calibrated and validated using field measurements obtained from the Westray Firth and Pentland Firth, as depicted in Fig. 2. These locations are characterized by natural channels that facilitate the acceleration of waters and winds from the Atlantic Ocean and are notable for strong coexistence of waves and currents. The field measurements collected at the Westray Firth are recorded by a 600 kHz Nortek AWAC unit with 3 slanted and 1 vertical beam to facilitate both wave and current measurements [12]. This instrument is mounted at the sea bottom and the mean water level at this site is around 52 m.

Similarly, the field measurements at Pentland Firth were recorded using the Teledyne Sentinel V50, a bed-mounted 5-beam ADCP, which was one of the ADCPs used in the MeyGen Phase 1a project [19], with details provided in publication [20]. The water depth of this location is around 37 m and the data were made available to this work by MeyGen. It is noticeable that there is no direct wave measurement from the Pentland Firth site. Instead, wave parameters were derived from the observed surface elevation using the spectra moment method, as reported in publication [20].

B. Numerical models

1) TOMAWAC wave model overview

The TOMAWAC module (version 8.1) [14] is used to simulate wave propagation. It solves the wave action balance equation for infinite or finite water depth, which is described by

$$\frac{\partial N}{\partial t}+\frac{\partial(\dot{x}N)}{\partial x}+\frac{\partial(\dot{y}N)}{\partial y}+\frac{\partial\left(\dot{k_x}N\right)}{\partial k_x}+\frac{\partial\left(\dot{k_y}N\right)}{\partial k_y}=Q\left(k_x,k_y,x,y,t\right) \quad (1)$$

where, N is the directional spectrum of wave action density; (x,y) is the spatial location in the Cartesian coordinates system, and the $\dot{x}$ and $\dot{y}$ are the transfer rate denoting the spatial propagation of wave energy; (k_x,k_y) represent the wave number vector for directional spectrum discretisation, which is defined by

$$k_x = k \cdot \sin\theta \tag{2}$$

$$k_y = k \cdot \cos\theta \tag{3}$$

in which k is the wave number and θ denotes the wave propagation direction; Q is the source or sink term, which represents the contributions of the following terms:

$$Q = Q_{in} + Q_{ds} + Q_{nl} + Q_{bf} + Q_{br} + Q_{tr} + Q_{ds,cur} + Q_{veg} + Q_{porous} \tag{4}$$

in which, Q_{in} is wind input for wave generation, Q_{ds} is white capping induced interactions, Q_{nl} is non-linear quadruplet interactions, Q_{bf} is bottom friction induced energy dissipation, Q_{br} is bathymetric breaking induced energy dissipation, Q_{tr} is non-linear triad interactions, $Q_{ds,cur}$ is enhanced breaking dissipation of waves on a current, Q_{veg} is dissipation due to vegetation, and Q_{porous} is dissipation due to porous media.

2) TELEMAC 3D flow model overview

The TELEMAC 3D module (version 8.1) [15] is a three-dimensional (3D) computational code describing the 3D velocity field, which is utilised for tidal current simulation in this research. The TELEMAC 3D solves the 3D Navier-Stokes equations with a free surface, which is expressed by,

$$\frac{\partial u}{\partial x} + \frac{\partial v}{\partial y} + \frac{\partial w}{\partial z} = 0 \tag{5}$$

$$\frac{\partial u}{\partial t} + u\frac{\partial u}{\partial x} + v\frac{\partial u}{\partial y} + w\frac{\partial u}{\partial z} = -g\frac{\partial u}{\partial x} + \upsilon\Delta(u) + F_x \tag{6}$$

$$\frac{\partial v}{\partial t} + u\frac{\partial v}{\partial x} + v\frac{\partial v}{\partial y} + w\frac{\partial v}{\partial z} = -g\frac{\partial v}{\partial x} + \upsilon\Delta(v) + F_y \tag{7}$$

$$p = p_{atm} + \rho_0 g(z_s - z) + \rho_0 g\int_z^{z_s}\frac{\Delta\rho}{\rho_0}dz' \tag{8}$$

in which, u, v, and w are the three-dimensional components of velocity; x, y and z are the 3D coordinates, g is the gravity acceleration, υ is the kinematic viscosity, F_x and F_y are the source terms (which in this research are the wave driving force), p and p_{atm} are the total pressure and atmospheric pressure respectively, z_s is the free surface elevation, ρ_0 and $\Delta\rho$ are the reference density and the variation of density around it respectively.

III. MODEL SET-UP

C. North Atlantic Ocean-scale TOMAWAC wave model

The large-scale wave model that covers the British Isles and the North Atlantic region was constructed in TOMAWAC to simulate wave parameters. The longitude of the simulation domain ranges from 10°E to 75°W and latitude ranges from 9°N to 70°N, as shown in Fig. 1 (a). The unstructured triangular mesh and boundary conditions are generated and defined by BlueKenue [21], in which the data sources of the geometry information, including coastlines/shorelines and bathymetry, are given in Table II. The spatial and temporal 10 m surface wind that drives the wave model was extracted from the ERA5 hourly data provided by the European Centre for Medium-Range Weather Forecasts (ECMWF) [22]. Regarding the wave spectrum being simulated, the number of wave directions is set to 36; the number of wave frequencies set for the wave model is 36 with the minimum frequency of 0.04 Hz and frequent ratios of 1.1. The time step of the wave model is set to 600 s. During the simulation, currents are not considered, while the energy dissipation due to the bottom friction Q_{bf}, depth-induced wave breaking Q_{br}, and white capping Q_{ds} is into account.

In order to derive the wave boundaries for the small-scale model, it is required to input the corresponding boundary coordinates. Upon completion of the simulation, the spatial and temporal wave spectrums at the required coordinates is generated and packaged to a result file. This output file can then be utilized as an input for other simulation cases.

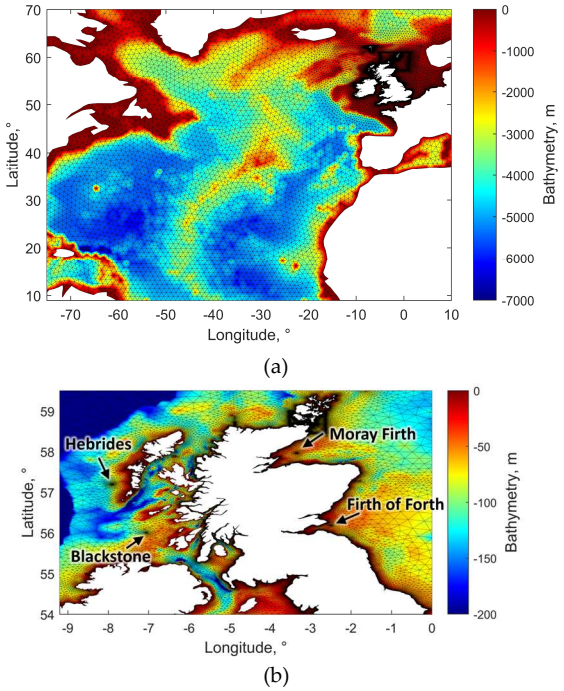

Fig. 1. Bathymetry and geometric mesh of the TOMAWAC wave model: (a) simulation domain and (b) zoomed-in version showing the locations of four Cefas WaveNet buoys

D. *Small scale flow model and wave-current coupled model*

The TELEMAC 3D flow model and TOMAWAC and TELEMAC 3D coupled model (also referred to TOM-TEL model in this paper) share the same unstructured triangular geometric mesh, of which the boundary conditions and rely on the same software and database as aforementioned. The simulation domain is defined by the UTM coordinates of zone 30, ranging from 391477.250 to 6559621.500 in the east direction and from 634525.000 to 6770000.000 in the north direction, as Fig. 2 shows. This domain covers both the PFOW region and the Shetland Islands (see Fig. 2 (a)) to ensure sufficient space for wave propagation in the TOM-TEL coupled model. By setting larger mesh lengths outside the PFOW region and using a relatively small number of mesh elements, the simulation time is negligibly affected compared to a simulation limited to the PFOW region alone.

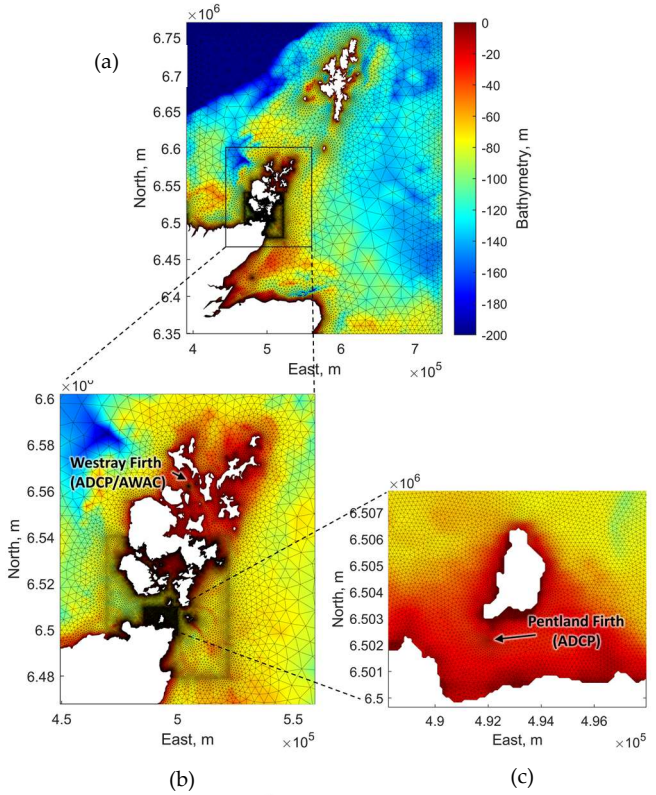

Fig. 2. Bathymetry and geometric mesh of the TELEMAC 3D model and TOM-TEL coupled model: (a) simulation domain, (b) zoomed-in version of the PFOW, and (c) zoomed-in version of the Pentland Firth area.

Given the primary focus of this study on the mean flow speed and surface waves, the number of vertical layers in this case has been set to 4 to optimize simulation efficiency. These layers consist of the bottom and free surface, forming the first and last layers respectively, while two additional fixed depth layers are incorporated in between to align with the field measurement. The boundary conditions are set to the open boundary with prescribed water level, and the TPXO9 tidal model is applied as the tidal database. The horizontal turbulence model employs a constant viscosity coefficient with a default value of 10^{-6}, while the vertical turbulence model is implemented using the mixing length method of TELEMAC 3D [15]. After a parameter study, the law of bottom friction is set to the Chézy formulation with a constant value of 66 to the entire computational domain and the coefficient to calibrate tidal range is set to 1.4.

The capability to conduct interactive simulations between TOMAWAC and TELEMAC 3D is provided by their integration within the same software, which can be achieved through the definition of a set of parameters outlined in their manuals [14], [15]. This study employs a bi-directional coupling approach between TOMAWAC and TELEMAC 3D (see Fig. 3), in which updated values of current velocity and water depth are transmitted from TELEMAC 3D to TOMAWAC. Subsequently, TOMAWAC solves the wave action density conservation equation with respect to these updated values of current and water depth and returns the corresponding updated values of wave driving forces F_x and F_y acting on the current to TELEMAC 3D [14]. The energy dispassion sources are set similar as the North Atlantic model with the only difference that the dissipation by strong current is enable. The flow model has a time step of 5 seconds. The coupling period between wave and flow model is 600 s, which is the same as the time step of wave model.

TABLE II
KEY DATABASE APPLIED IN TOMAWAC AND OR TELEMAC 3D NUMERICAL MODELS

Name	Database	Remark
Coastlines	GSHHGD [23]	-
Bathymetry	GEBCO [24]	Release in 2020
Wind	ECMWF ERA5 [22]	1 hour interval, 0.25° x 0.25° resolution
Tidal models	TPXO9 version 4 [25]	Release in 2020

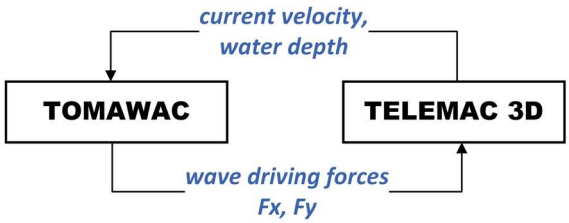

Fig. 3. Bi-directional simulation of the TOMAWAC and TELEMAC 3D coupled model.

IV. MODEL CALIBRATION AND VALIDATION

E. *North Atlantic-scale TOMAWAC wave model results*

The model calibration time is May 2015 and the model validation period is July and August 2016. Fig. 4 shows the calibration simulation results at four Cefas Wavenet buoys sites of the North Atlantic Ocean-scale TOMAWAC wave model against measurement in May 2015. The correlation coefficients (R) between the simulation results and measurement of significant wave heights H_{m0} at two west coast sites (i.e. facing Atlantic),

Hebrides and Blackstone, are more than 97% with small values of the root mean square error (RMSE) and scatter index (SI). In the meantime, the R value of zero-crossing wave periods T_m and peak wave periods T_p at those locations are more than 83% and 50% respectively, which indicates this wave model performs very well in west coast area. While for Moray Firth and Firth of Forth, the R values of H_{m0} is higher than 87%, and of T_m and T_p are more than 71% and 47%, it is still showing good estimation of wave parameters. Table III presents the validation results of H_{m0} and T_p in July and August 2016. Notably, while T_m is also simulated and validated against measurements, only the results for T_p are presented in this context due to the greater challenge of achieving a precise match with the measurements. Once again, Hebrides and Blackstone exhibit high R values of over 96% for H_{m0} and over 83% for T_p, and Moray and Forth Firth produce slightly lower but still acceptable results. The superior performance of Hebrides and Blackstone locations is likely due to the North Atlantic's ample space for wave propagation, in contrast to the more confined areas of Moray Firth and Firth of Forth.

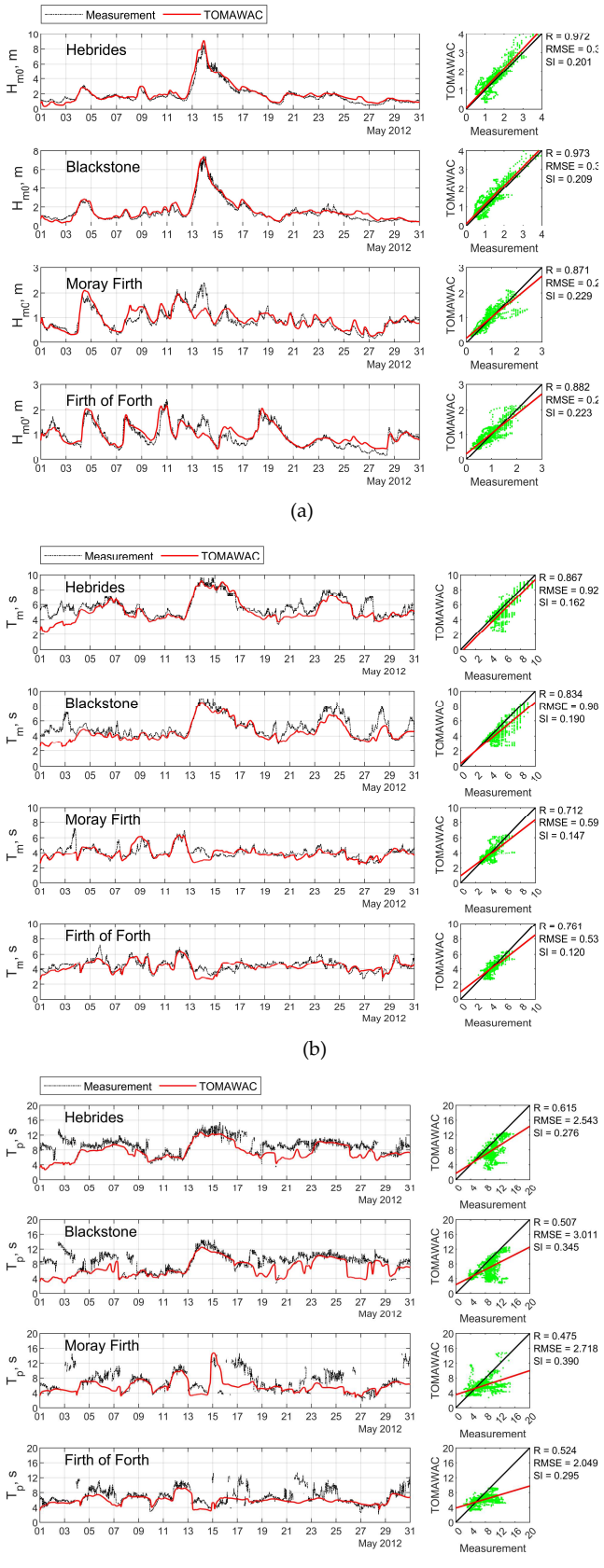

Fig. 4. Calibration results of (a) significant wave heights, (b) zero-crossing wave periods, (c) and peak wave periods of the North Atlantic Ocean-scale TOMAWAC wave model in May 2012 against the measurement by Cefas WaveNet buoys (time series on the left, scatter plots on the right)

The open-sourced TOMAWAC model demonstrates similar quality results as the MIKE 21 model used in a comparable study by Venugopal [3] at the same locations and periods (May 2012).

TABLE III
SIGNIFICANT WAVE HEIGHTS AND PEAK WAVE PERIODS VALIDATION RESULTS AT CEFAS WAVENET BUOYS OF THE NORTH ATLANTIC OCEAN-SCALE TOMAWAC WAVE MODEL IN JULY AND AUGUST 2016.

Site	Wave Parameters	RMSE	SI	R
Hebrides	H_{m0} (m)	0.135	0.270	0.976
	T_p (s)	0.118	1.067	0.851
Blackstone	H_{m0} (m)	0.288	0.164	0.961
	T_p (s)	1.122	0.129	0.835
Moray Firth	H_{m0} (m)	0.307	0.197	0.805
	T_p (s)	0.452	2.544	0.632
Firth of Forth	H_{m0} (m)	0.169	0.313	0.856
	T_p (s)	2.476	0.427	0.523

F. TELEMAC 3D tidal flow model results

The calibration of the three-dimensional TELEMAC 3D tidal flow model was carried out at the Westray Firth site from 28 July to 31 August 2016, while the validation was performed at the Pentland Firth site from 1 to 30 November 2017. The model's performance was evaluated by comparing its simulated tidal flow velocity at two fixed water depths with the AWAC or ADCP measurements, as shown in Fig. 5 and 6, respectively. The results demonstrate a strong correlation between the model's simulated east velocity (U) and north velocity (V), with R values exceeding 98%, and minimal root mean square error (RMSE) and scatter index (SI) across all cases. These findings affirm the effectiveness of the flow model.

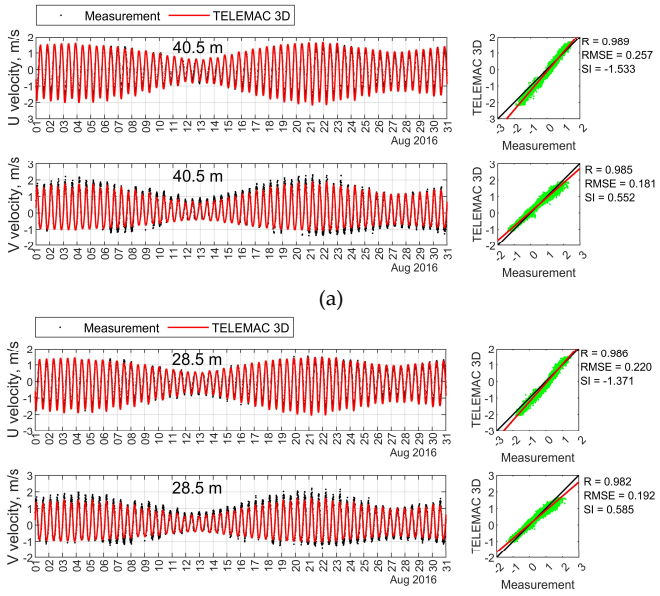

(a)

(b)

Fig. 5. Comparison of tidal flow velocity components (U: east direction, V: north direction) at two fixed depths (a) 40.5 m and (b) 28.5 m from sea bottom: AWAC measurement vs. TELEMAC 3D tides-only model in Westray Firth, August 2016 (time series on the left, scatter plots on the right)

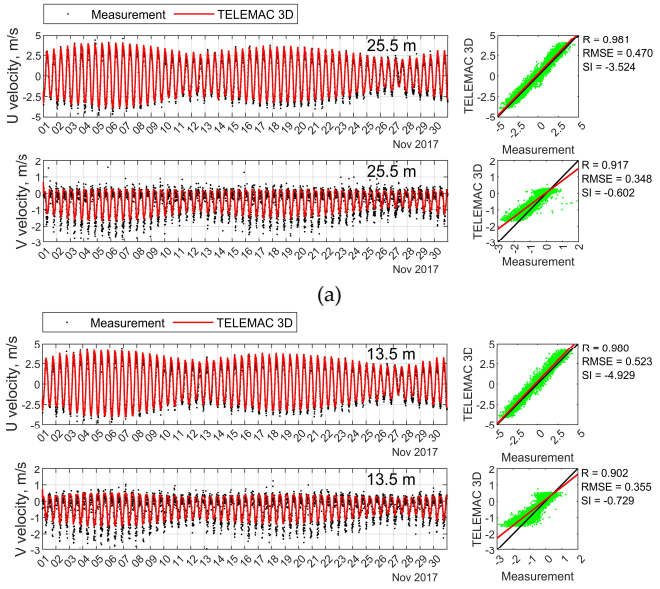

(a)

(b)

Fig. 6. Comparison of tidal flow velocity components (U: east direction, V: north direction) at two fixed depths (a) 25.5 m and (b) 13.5 m from sea bottom: ADCP measurement vs. TELEMAC 3D tides-only model in Pentland Firth, November 2017 (time series on the left, scatter plots on the right)

G. *TOM-TEL wave-current coupled model results*

The calibration and validation results of H_{m0} and T_m of the TOM-TEL coupled model at Westray Firth and Pentland Firth are depicted in Fig. 7 (a) and (b). It is notable that the H_{m0} and T_m field measurements at these sites display regular fluctuations compared to the flat data observed by Cefas Wavenet buoys (see Fig.4 for locations where waves dominated) indicating the modulation of waves by periodic tidal currents. The simulation results of the coupled model closely follow these fluctuations, with R values ranging from 71% to 92% for fluctuating H_{m0} and T_m at Westray Firth, demonstrating the successful consideration of wave-current interaction and its accurate representation. In the case of Pentland Firth, while the R values for wave heights may not be as high as Westray Firth (81%), it is important to note that the wave height measurement is derived from surface elevation calculation, which is prone to the amplification of flow turbulence or environmental noise into the wave results. Despite this potential source of error, the shape of the results closely matches the measured values and an R value above 80% is still considered to be acceptably good.

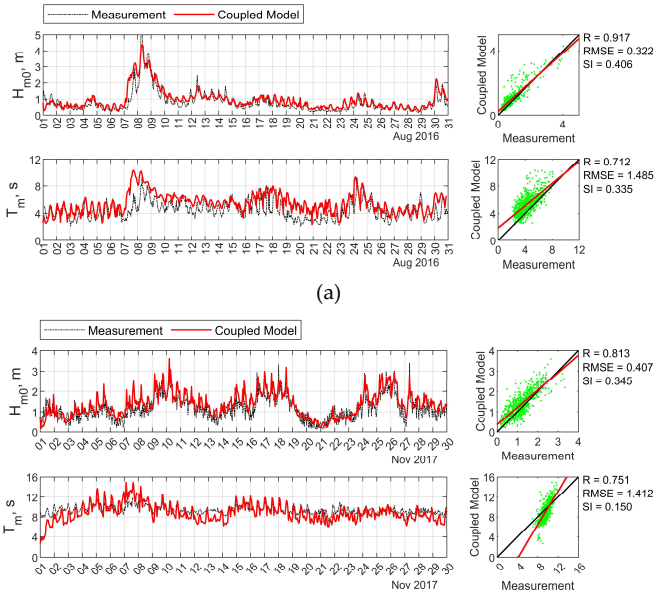

(a)

(b)

Fig. 7. Comparison of significant wave heights and zero-crossing wave periods in (a) Westray Firth, August 2016 and (b) Pentland Firth, November 2017: AWAC or ADCP measurement vs. TOM-TEL wave-current coupled model (time series on the left, scatter plots on the right

V. WAVE-CURRENT INTERACTIONS

By comparing the simulation results of the numerical models discussed earlier, the effects of wave-current interactions on wave and current parameters can be analysed qualitatively and quantitatively. Fig. 8 (a) and 9 (a) exhibit the current and wave simulation results of the TELEMAC 3D flow model, TOMAWAC wave model, and TOM-TEL coupled model at the Westray Firth and Pentland Firth locations in November 2017, respectively. The first two subplots of Fig. 8 (a) and 9 (a) display the mean current speeds and their corresponding current directions, indicating a negligible difference between the current-only model and wave-current coupled model. In most cases, both models yield almost the same current parameters. This is probably due to the time step of the wave simulation (every 600 s) is much larger than that of the tidal current simulation (every 5 s). As a result, the

effects of wave-current interactions on tidal current within 600 s are hardly observed. A similar phenomenon has been found in the Fig. 9 of [26]. This is the possible limitation of numerical modelling, which is not able to simulate the wave-current interactions at every moment current is simulated, if the time step for wave simulation is higher than that of the tide.

On the contrary, the current has a significant influence on wave parameters. The simulation results of the wave-current coupled model, as shown in Fig. 8 and 9, demonstrate clear periodic fluctuations in the mean wave direction, H_{m0}, T_m, and the wave spread compared to the wave-only model, which follows a similar pattern to the tidal cycle. This phenomenon indicates that wave is modulated by tidal current. The underlying factors contributing to this phenomenon include wave refraction resulting from waves propagating over spatially varying currents, as well as conservation of wave action. The latter can lead to an increase in wave height as waves encounter opposing currents, leading to wave steepening and ultimately wave breaking [26], [27]. The results have furtherly proved this, as the maximum H_{m0} is been considerably raised after introducing currents, with an increase from 4 m to 4.5 m at Westray location and 2.8 m to 3.6 m at Pentland Firth location. This occurs when the wave and current are in the same direction. Another evidence is shown in Fig. 8 (b), which has revealed the angle difference of the wave direction and current direction

$$Angle\ diff. = abs(wave\ direction - tidal\ direction) \tag{9}$$

at local extremum points of H_{m0} results (shown by black square marker). Local extrema points are found by using MATLAB's "findpeaks" function with Minimum Peak Distance set to half a day. At the Pentland Firth site, for 47 local extremum points detected, all of them to a very small direction difference which is within around 30 degrees. This means wave and current are within a small angle, or can be seen as almost same directions of movement.

Similar phenomena are found in Westray Firth site before 21 November, which 25 local peaks of the H_{m0} refers to small angle difference between waves and tides.

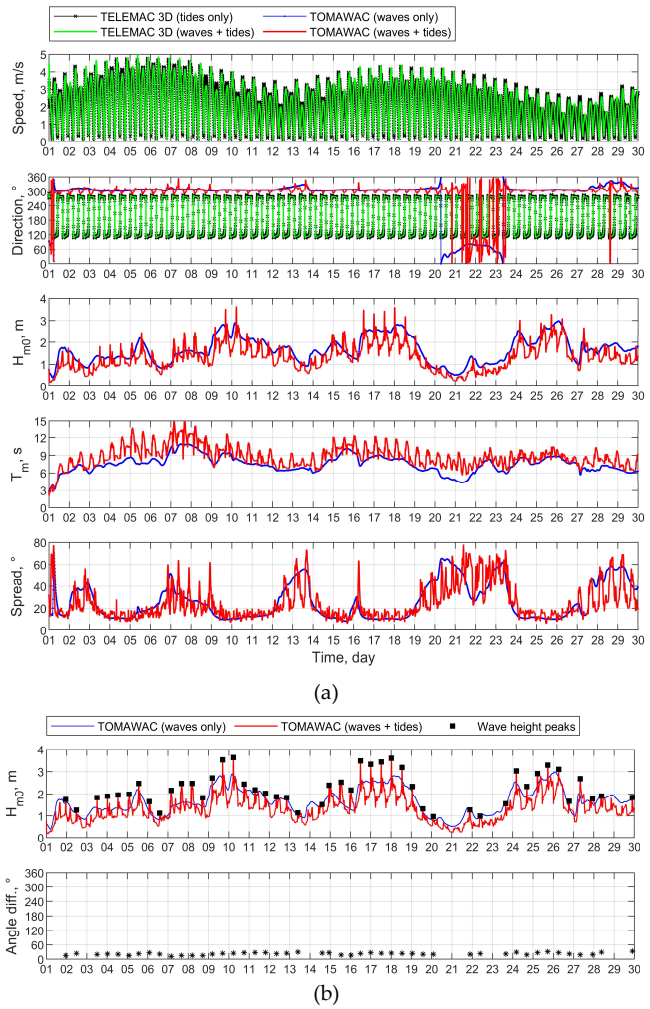

Fig. 8. Comparison of mean flow speed, tidal and incoming wave directions, significant wave heights, zero-crossing wave periods, and wave spread among the tides-only, waves-only, and wave-current coupled model (a), and the absolute angle difference between wave and tidal directions when the wave heights of the coupled model at local extremum points (b) at Pentland Firth site in November 2017.

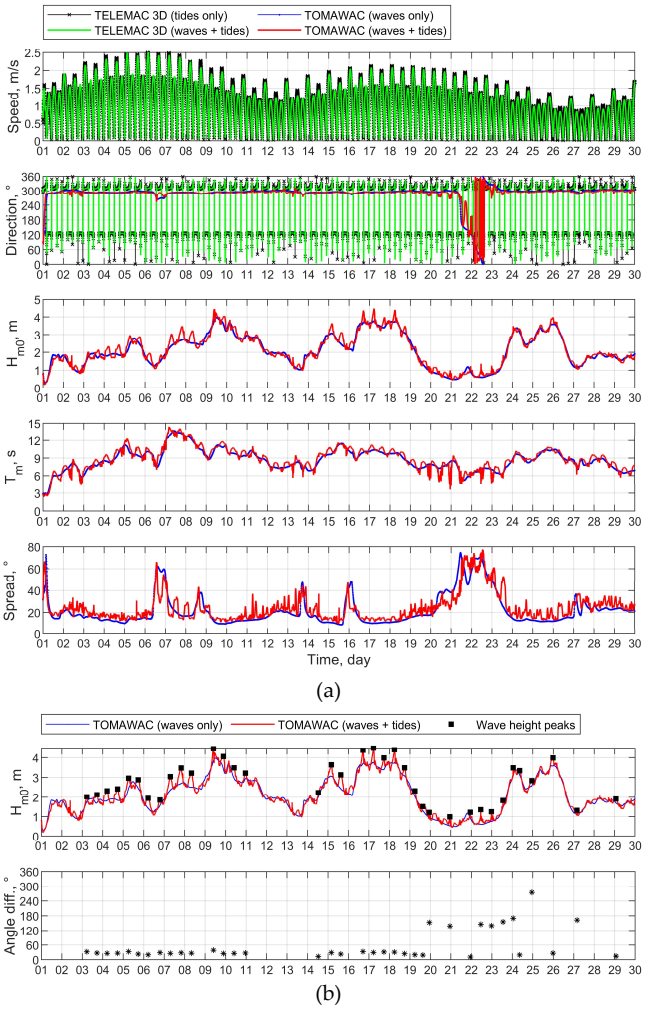

Fig. 9. Comparison of mean flow speed, tidal and incoming wave directions, significant wave heights, zero-crossing wave periods, and wave spread among the tides-only, waves-only, and wave-current coupled model (a), and the absolute angle difference between wave and tidal directions when the wave heights of the coupled model at local extremum points (b) at Westray Firth site in November 2017.

For the exceptions during 21 to 25 November, which is highly possible due to the significant fluctuation of wave direction because of the extreme changes of winds and wave-current interactions. Overall, in November 2017, the coupled model show a 25.19% increase in wave heights at Pentland Firth and 20.47% increase at Westray Firth when the angle between the wave and the tide is small.

Similar phenomenon can also be found in the zero-crossing wave periods and wave spread. When wave and current are in the same direction, T_m increase and wave spread value decrease.

VI. Conclusion

Three types of numerical model were established using the sub-modules of the open-sourced CFD software TELEMAC-MASCARET. These models include: 1) North Atlantic Ocean-scale TOMAWAC wave model, 2) Scotland-scale TELEMAC 3D tidal flow model, and 3) Scotland-scale TOMAWAC and TELEMAC 3D wave-current coupled model. The wave-only model was calibrated and validated with the observations from the Cefas WaveNet buoys, while the current-only model and wave-current coupled model were verified with the AWAC measurement at Westray Firth and ADCP field data at Pentland Firth. All three models were found to be in good agreement with real-world observations.

Through the use of these models, the effects of wave-current interactions on various parameters are investigated. By comparing the results of the coupled model to the flow model, the tidal parameters seems to be rarely affected by the interactions, likely due to the limitation of the numerical modelling that no wave effects is into account within the time step of wave simulation (i.e. 600 s in this study). In contrast, current modulations in wave parameters were clearly observed. This phenomenon can be attributed to conservation of wave action, which can lead to an increase in wave heights as waves encounter opposing currents, ultimately resulting in wave steepening and breaking. Specifically, in Pentland Firth site, it was found that the wave height of local peak values is raised by 25.19% to the wave-only model, while for Westray Firth site, it increased by 20.47%. Similar phenomena were observed in wave periods and wave spreads.

The numerical models developed in this study are valuable tools for generating wave boundary conditions, predicting waves or tides, and assessing marine energy resource. The analysis of wave-current interactions provides a quantitative assessment of their effects on important wave parameters and is expected to assist engineers in designing projects that can safely operate in a wave-current environment.

References

[1] S. P. Neill, M. J. Lewis, M. R. Hashemi, E. Slater, J. Lawrence, and S. A. Spall, "Inter-annual and inter-seasonal variability of the Orkney wave power resource," *Applied Energy*, vol. 132, pp. 339–348, Nov. 2014, doi: 10.1016/j.apenergy.2014.07.023.

[2] G. Lavidas, V. Venugopal, and D. Friedrich, "Wave energy extraction in Scotland through an improved nearshore wave atlas," *International Journal of Marine Energy*, vol. 17, pp. 64–83, Apr. 2017, doi: 10.1016/j.ijome.2017.01.008.

[3] V. Venugopal and R. Nemalidinne, "Wave resource assessment for Scottish waters using a large scale North Atlantic spectral wave model," *Renewable Energy*, vol. 76, pp. 503–525, Apr. 2015, doi: 10.1016/j.renene.2014.11.056.

[4] S. Draper, T. A. A. Adcock, A. G. L. Borthwick, and G. T. Houlsby, "Estimate of the tidal stream power resource of the Pentland Firth," *Renewable Energy*, vol. 63, pp. 650–657, Mar. 2014, doi: 10.1016/j.renene.2013.10.015.

[5] A. Perez Ortiz, *A Systematic Approach to Undertake Tidal Energy Resource Assessment with Telemac-2D*. 2013.

[6] S. Baston and R. E. Harris, "Modelling the Hydrodynamic Characteristics of Tidal Flow in the Pentland Firth,"

[7] S. Waldman, S. Bastón, R. Nemalidinne, A. Chatzirodou, V. Venugopal, and J. Side, "Implementation of tidal turbines in MIKE 3 and Delft3D models of Pentland Firth & Orkney Waters," *Ocean & Coastal Management*, vol. 147, pp. 21–36, Oct. 2017, doi: 10.1016/j.ocecoaman.2017.04.015.

[8] S. P. Neill, M. R. Hashemi, and M. J. Lewis, "The role of tidal asymmetry in characterizing the tidal energy resource of Orkney," *Renewable Energy*, vol. 68, pp. 337–350, Aug. 2014, doi: 10.1016/j.renene.2014.01.052.

[9] A. Abdul Rahman and V. Venugopal, "Inter-Comparison of 3D Tidal Flow Models Applied To Orkney Islands and Pentland Firth," Sep. 2015.

[10] R. O'Hara Murray and A. Gallego, "A modelling study of the tidal stream resource of the Pentland Firth, Scotland," *Renewable Energy*, vol. 102, pp. 326–340, Mar. 2017, doi: 10.1016/j.renene.2016.10.053.

[11] A. Saruwatari, D. M. Ingram, and L. Cradden, "Wave–current interaction effects on marine energy converters," *Ocean Engineering*, vol. 73, pp. 106–118, Nov. 2013, doi: 10.1016/j.oceaneng.2013.09.002.

[12] V. Venugopal, A. Vögler, and B. Sellar, "Characterisation of Wave-Tidal Current-Turbulence Interactions at Tidal Energy Sites in the Orkney Islands," presented at the The 28th International Ocean and Polar Engineering Conference, OnePetro, Jun. 2018. Accessed: Oct. 11, 2022. [Online]. Available: https://onepetro.org/ISOPEIOPEC/proceedings/ISOPE18/All-ISOPE18/ISOPE-I-18-240/20382

[13] V. Venugopal and R. Nemalidinne, "Marine Energy Resource Assessment for Orkney and Pentland Waters With a Coupled Wave and Tidal Flow Model," in *Volume 9B: Ocean Renewable Energy*, San Francisco, California, USA: American Society of Mechanical Engineers, Jun. 2014, p. V09BT09A010. doi: 10.1115/OMAE2014-24027.

[14] T. Awk, "TOMAWAC user manual version 8.1," *The TELEMAC-Mascaret Consortium*, vol. 7, no. 3, 2019.

[15] T. Awk, "TELEMAC 3D user manual version 8.1," *The TELEMAC-Mascaret Consortium*, vol. 7, no. 3, 2019.

[16] "open TELEMAC-MASCARET." http://www.opentelemac.org/ (accessed Aug. 17, 2022).

[17] N. Guillou, "Evaluation of wave energy potential in the Sea of Iroise with two spectral models," *Ocean Engineering*, vol. 106, pp. 141–151, Sep. 2015, doi: 10.1016/j.oceaneng.2015.06.033.

[18] "Cefas - WaveNet interactive map." https://wavenet.cefas.co.uk/Map (accessed May 10, 2023).

[19] MeyGen, "MeyGen," *SIMEC ATLANTIS ENERGY*, 2018. https://simecatlantis.com/tidal-stream/meygen/ (accessed Aug. 17, 2022).

[20] D. Coles, C. Greenwood, A. Vogler, T. Walsh, and D. Taaffe, "Assessment of the turbulent flow upstream of the Meygen

Phase 1A tidal stream turbines," *Proceedings of the Asian Wave and Tidal Energy Conference, Taipei, Taiwan.*, Sep. 2018.

[21] N. R. C. Canada, "Blue Kenue™: software tool for hydraulic modellers," Mar. 19, 2019. https://nrc.canada.ca/en/research-development/products-services/software-applications/blue-kenuetm-software-tool-hydraulic-modellers (accessed May 10, 2023).

[22] "Copernicus Climate Change Service (C3S)," *ERA5: Fifth generation of ECMWF atmospheric reanalyses of the global climate . Copernicus Climate Change Service Climate Data Store (CDS)*, 2017. https://cds.climate.copernicus.eu/cdsapp#!/home (accessed Aug. 17, 2022).

[23] P. Wessel and W. H. Smith, "A global, self-consistent, hierarchical, high-resolution shoreline database," *Journal of Geophysical Research: Solid Earth*, vol. 101, no. B4, pp. 8741–8743, 1996.

[24] GEBCO Bathymetric Compilation Group 2020, "The GEBCO_2020 Grid - a continuous terrain model of the global oceans and land." British Oceanographic Data Centre, National Oceanography Centre, NERC, UK, Apr. 28, 2020. doi: 10.5285/a29c5465-b138-234d-e053-6c86abc040b9.

[25] G. D. Egbert and S. Y. Erofeeva, "Efficient Inverse Modeling of Barotropic Ocean Tides," *Journal of Atmospheric and Oceanic Technology*, vol. 19, no. 2, pp. 183–204, Feb. 2002, doi: 10.1175/1520-0426(2002)019<0183:EIMOBO>2.0.CO;2.

[26] A.-C. Bennis *et al.*, "Numerical modelling of three-dimensional wave-current interactions in complex environment: Application to Alderney Race," *Applied Ocean Research*, vol. 95, p. 102021, Feb. 2020, doi: 10.1016/j.apor.2019.102021.

[27] L. Romero, L. Lenain, and W. K. Melville, "Observations of Surface Wave–Current Interaction," *Journal of Physical Oceanography*, vol. 47, no. 3, pp. 615–632, Mar. 2017, doi: 10.1175/JPO-D-16-0108.1.